Proceedings of International Design Engineering Technical Conferences & Computers and Information in Engineering Conference
IDETC-CIE
August 17, 2025, Anaheim, California

SELF-CONTAINED ELECTRICAL CONDUCTIVITY SENSING SPIKES FOR MONITORING OF LEVEE WETTING AND DRYING CYCLES

Sydney Morris
Department of
Mechanical Engineering
University of South Carolina
Columbia, South Carolina 29208
Email: slm30@email.sc.edu

Ayman Mokhtar Nemnem
Department of
Civil and Environmental Engineering
University of South Carolina
Columbia, South Carolina 29208
Email: amokhtar@email.sc.edu

Malichi Flemming
Department of
Mechanical Engineering
University of South Carolina
Columbia, South Carolina 29208
Email: malichi@email.sc.edu

Austin R.J. Downey
Department of
Mechanical Engineering
Department of
Civil and Environmental Engineering
University of South Carolina
Columbia, South Carolina 29208
Email: austindowney@sc.edu

Puja Chowdhury
Department of
Mechanical Engineering
University of South Carolina
Columbia, South Carolina 29208
Email: pujac@email.sc.edu

Matthew Burnett
Department of
Mechanical Engineering
University of South Carolina
Columbia, South Carolina 29208
Email: matthew.burnett@sc.edu

Jasim Imran
Department of
Civil and Environmental Engineering
University of South Carolina
Columbia, South Carolina 29208
Email: imran@sc.edu

Sadik Khan
Department of
Civil and Environmental Engineering
and Industrial Systems and Technology
Jackson State University
Jackson, Mississippi 39217
Email: sadik.khan@jsums.edu

ABSTRACT

Levees are earthen structures built parallel to water bodies, such as rivers, to protect important infrastructure, assets, and people from flooding. They play a critical role in protecting lives, but their structural integrity is frequently threatened by lack of maintenance leading to moisture-induced degradation. Traditional levee monitoring systems can be expensive due to the need for extensive sensor networks across vast areas. To address this, there is a growing need for low-cost sensing solutions that can provide data without requiring dense sensor coverage. Direct measurements of subsurface parameters, such as soil saturation levels, are helpful for accurately assessing the structural health of levees, as these measurements provide real-time insights into the moisture conditions that can weaken soil strength and lead to potential failures. This study investigates the application of newly developed self-contained sensing spikes, equipped with electrical conductivity sensors that embed themselves 13 cm below the surface, designed to monitor wetting and drying

cycles within levee soils. In a controlled and monitored 144-hour flume test, six spikes were strategically placed on a 0.45-meter-high sand embankment as water levels were raised and lowered to capture conductivity changes over time. Using the B-spline method, a map of conductivity was constructed, providing a graphical representation of moisture distribution across the levee. This non-linear mapping technique allows for accurate detection of moisture-driven faults with significantly fewer sensors, demonstrating that under-sampling can achieve reliable monitoring results. The embedded conductivity sensors enable continuous, low-cost monitoring of moisture dynamics directly at critical depths, offering a novel approach to detecting levee faults and predicting potential bank erosion. By linking conductivity data to fragility assessments, this method enhances the ability to forecast structural vulnerabilities, contributing to improved levee resilience and maintenance strategies under changing environmental conditions.

1 INTRODUCTION

Levees, protective earthen structures, are built directly beside water bodies, leaving them at risk for damage. Levee failure is an ongoing threat, commonly onset by natural disasters such as heavy rain, flooding, hurricanes, and earthquakes [1, 2]. This can lead to a series of breaks: overtopping can occur when flooding increases water levels and causes them to rise above the levee's peak, resulting in erosion; seepage can occur when water traveling subsurface to the levee displaces the earthen materials, creating inner channels [3]. While levees can disrupt the momentum of hurricanes, direct physical impacts from those and earthquakes can cause the structures to fail [2].

Furthermore, burrowing mammals are another natural disaster that imposes threats to levees as the animals find the embankments hospitable [4]. When the mammals dig into the levee, they create tunnels that emulate the effects of seepage and undermine the structural integrity of the structure. This bioerosion allows for an influx of water through the levee, putting the protected side at risk of flooding [4].

Electrical conductivity (EC) is the measure of the ability of water to pass an electrical current. This can be due to two factors: salinity content and temperature. As both factors increase, so does conductivity. Salinity affects conductivity because inorganic compounds carry higher charges than organic compounds [3]. Temperature affects conductivity because ion mobility increases proportionally as liquid viscosity decreases and molecules are able to dissociate [5]. This is why electrical conductivity sensors are a viable option for predicting levee failure and monitoring their overall health. Outdoor water sources have higher concentrations of conductive compounds than purified water so they can be measured. This paper will focus on the longer-term application of this sensing capability.

While they are related, there is a difference between EC and conductance. Conductance is a direct measurement of how easily current can flow through a particular solution whereas EC is a generalized measure of electrical conduction with respect to geometry [5]. This difference, alongside comparing against total dissolved solids, becomes more noticeable when identifying certain solutions rather than simply evaluating a change in values [6].

The contributions of this work are twofold. First, a self-contained electrical conductivity sensing spike system is demonstrated for monitoring levee wetting and drying cycles. Second, B-spline interpolation is used to detect moisture-driven faults with fewer sensors, reducing monitoring costs.

2 METHODOLOGY

This section describes the sensor hardware and experimental setup used in this work.

2.1 HARDWARE

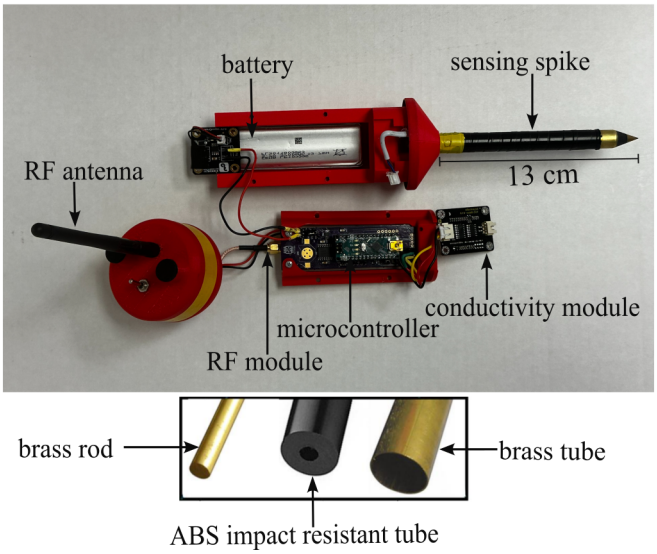

FIGURE 1. Dissected overview of all major components on the sensor package.

The hardware developed for this experiment builds off of prior works related to the sensor package [3] and its wireless versions [7].

The hardware is split into two parts: a wireless electrical conductivity sensing spike package and a receiver for data collection. These hardware designs are open-source and featured on a public Github repository under Columbia v0.6.0 [8].

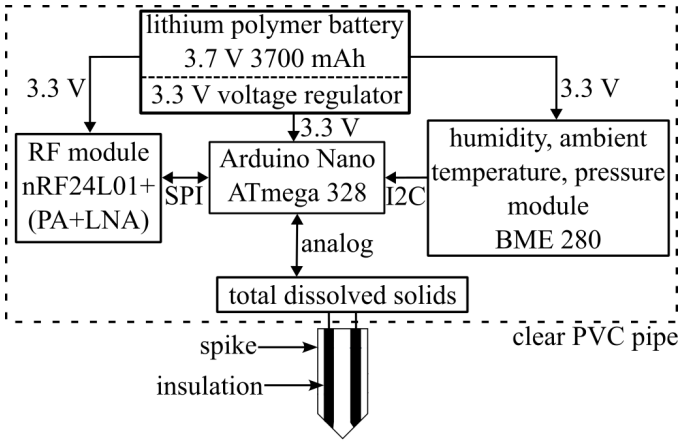

FIGURE 2. Functional block diagram showing major components of the sensor package.

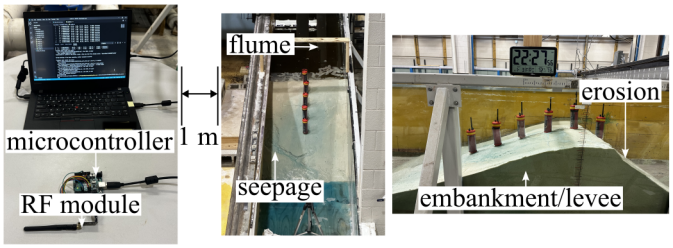

FIGURE 3. Various views of the experiment such as (a) the receiver station; (b) a head-on look at the embankment, featuring seepage; (c) a side look of the embankment.

The sensing spike package features a conductive brass spike that protrudes 13 cm from its base as shown in figure 1. The outer layer is wrapped in electrical tape so that the surface is only exposed at the tip, allowing for pinpointed location of data collection. An ABS tube is pressure-fitted for insulation so that the conductivity module has a reference point for recording data and is not subject to interference by touching connections. The package's main feature is its conductivity sensing ability, which is collected through the aforementioned spike design via a total dissolved solids (TDS) module.

Installed above the sensing spike, the package features approximately 5 inches of clear PVC pipe, waterproofed by rubber o-rings that have been pressure-fitted into the housing circumference. This PVC serves to protect the inner components, shown in figure 1, from the outer elements while maintaining a clear view of the inside. The protected housing stores the 3700 mAh 3.7 V lipo battery and the printed circuit board (PCB).

Figure 2 outlines the PCB's major components and connections. A microcontroller is the package's control base. Aside from the TDS, there is an RF transceiver module that allows for wireless data collection across distances. There is an environmental sensor in the form of a BME280 module, but it is for ambient internal readings in the housing rather than directly evaluating embankments, these internal readings include humidity, temperature, and pressure to ensure a stable environment within the package.

The RF module allows the receiver to communicate wirelessly with the sensing packages. This design uses the nRF24L01+ power-amplifier and low-noise amplifier (PA+LNA) module that includes an external antenna for farther distance communications up to 1000 unobstructed meters and enhanced signal handling [9]. One module is on every package and one module is used for the receiver. The RF modules use an octal network with six data pipes available per module [9], making this experiment the perfect number for a single module. The nRF24L01+ PA+LNA was chosen for its success in a previous wireless iteration [7]. The remaining components of the receiver station are the microcontroller and an active laptop with internet access (figure 3). The laptop gives a stable power supply to the base station rather than relying on a standalone battery and is the gateway to upload the data collection into a cloud-based shared drive from the sensors in real-time. The RF modules have been set to transmit a data packet every 10 seconds for precise real-time tracking.

2.2 EXPERIMENTAL SETUP

The experiment focuses on battery longevity and sensing data accuracy over an extended continuous time period, similar to if the package was realistically deployed in the field. Figure 4 displays an illustration of the setup. A 2-meter-long, 1-meter-wide earthen embankment is constructed within an indoor flume at the Hydraulics Laboratory at the University of South Carolina. The embankment has a right-side slope of 1:1 and a left-side slope of 3:1. Each spike is separated equidistantly from each other by 0.2 m to evenly distribute across the entire embankment, helping track as much area as possible. The flume fills with water on the right side to simulate a body of water. Notice that a single spike is positioned at water level to test the waterproofing; this is helpful in evaluating how well the housing stays intact in moments of submersion.

The setup is pictured in figure 3b and c. The receiver station is set up a meter away from the actual embankment to make use of the wireless transceiver ability. After the setup construction is complete, the experiment begins by initially filling the flume with water on the right side. The water is dyed orange to enhance its color and better visualize its paths throughout the levee. The water is then left beside the embankment for an hour before it is drained to begin the drying process. The drying process runs until the spikes lose battery power or stop transmitting

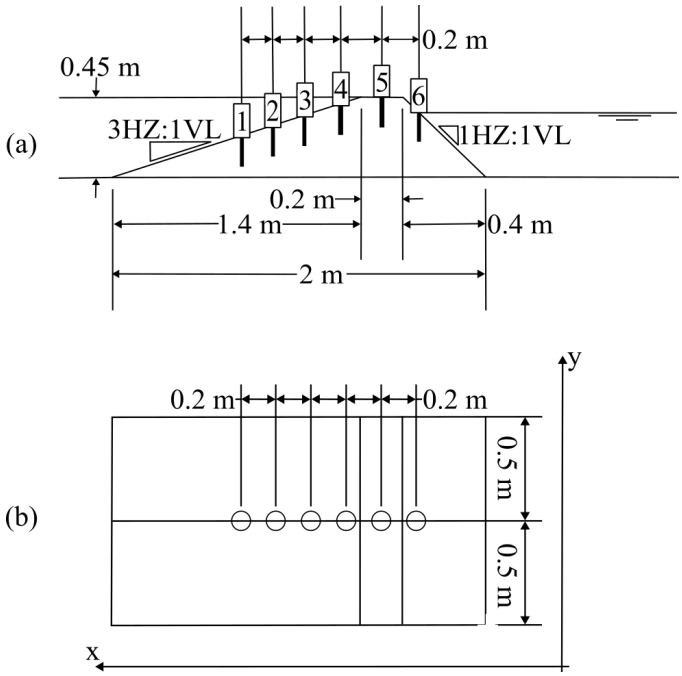

FIGURE 4. Cross-sectional view (a) and top-down view (b) of the experimental setup.

data, whichever comes first. Lasting approximately 127 hours on a full battery, the status of the spikes could easily be checked during this duration via the cloud-based network that it is synced to. This is afforded by the use of an active internet-connected laptop during the entire duration of the experiment.

2.3 BASIS SPLINES

Mathematically, B-splines (or basis splines) are generated by basis functions. A B-spline curve, $C(t)$, is given by

$$C(t) = \sum_{i=0}^{n} N_{i,k}(t) P_i, \tag{1}$$

where $N_{i,k}(t)$ are the basis functions of degree k, t is the parametric variable, and P_i are the shape-defining control points. The basis functions are defined recursively, starting with the base case ($k = 0$), and are defined as a piece-wise equation

$$N_{i,0}(t) = \begin{cases} 1, & t_i \leq t < t_{i+1}, \\ 0, & \text{otherwise.} \end{cases} \tag{2}$$

For $k > 0$, the basis functions follow the Cox de Boor recursion formula where t_i are knots from the knot vector

$$N_{i,k}(t) = \frac{t - t_i}{t_{i+k} - t_i} N_{i,k-1}(t) + \frac{t_{i+k+1} - t}{t_{i+k+1} - t_{i+1}} N_{i+1,k-1}(t). \tag{3}$$

Essentially, B-splines are a series of piece-wise functions; they follow a non-linear shape in the form of a polynomial of k degrees [10]. B-spline was chosen for its ability to smoothly fit non-linear models due to the knot feature that controls how the B-spline is divided over the entire dataset.

The code from the experimental receiver collects the value from the sensing spike in voltage which can be easily converted into various other units. Here, the dataset is converted to conductance, G, which is measured in siemens, S, using the following formula:

$$G = I/V, \tag{4}$$

where I is current (A) and V is voltage (V). Essentially, conductance is the inverse of resistance. While conductance and conductivity are notably different, it can easily be converted to EC with the proper medium calibration or conversion factor [5]. Assuming EC and voltage are linearly proportional, the values were converted to EC by empirically found calibration constants.

3 RESULTS AND DISCUSSION

Figure 5 shows an expanded view of each spike over time and figure 6 shows an overall graphical version of the dataset; table 2 provides the legend values for both figures. It is important to note how this graph, figure 6, should be read: each dot represents a specific spike at its respective location. Each position has a series of dots to represent that particular spike over time. It is a direct representation of the embankment setup. The data was interpolated using B-spline to better represent the changes in values. Although the experiment ran for a long period of time, the data changed at a slow rate.

Table 1 is an expanded subset of the data shown in figure 6. By displaying the experiment's start, the drying cycle and changes in conductivity over time can be better realized. Notice that the values never reach zero, which is attributed to the calibration of the sensing probe; therefore, a reading of 2.0 represents zero. This experiment is conducted as a part of a series of experiments; this experiment was conducted the following day to a previous one, leaving moisture present in the embankment at the experiment's start and thus giving two sensors a starting value above zero. This shows that this area of the embankment dries the slowest, which is further exemplified by spikes 1 and 2 holding EC for the longest time (figure 6). Spikes 1 and 2 are the closest to the bottom of the embankment. Therefore, the water is

TABLE 1. Sensor metrics where t is recorded in hours (h) and EC is recorded in microsiemens per centimeter (μS/cm).

node	x-coordinate (m)	y-coordinate (m)	$t = 0$	$t = 1$	$t = 24$	$t = 48$	$t = 72$	$t = 96$	$t = 120$	$t = 144$
1	1.35	0.5	20.0420	31.6546	25.2245	23.9396	23.6547	19.3276	19.3276	2.0
2	1.15	0.5	7.1434	29.0778	9.7562	8.4292	8.4292	8.4292	2.0	dead
3	0.95	0.5	2.0	29.0778	3.2858	2.0	3.2858	2.0	2.0	2.0
4	0.75	0.5	2.0	33.9236	2.0	2.0	2.0	2.0	2.0	2.0
5	0.55	0.5	2.0	29.0778	2.0	2.0	2.0	2.0	2.0	dead
6	0.35	0.5	2.0	52.2865	3.2858	3.2858	3.2858	3.2858	3.2858	2.0

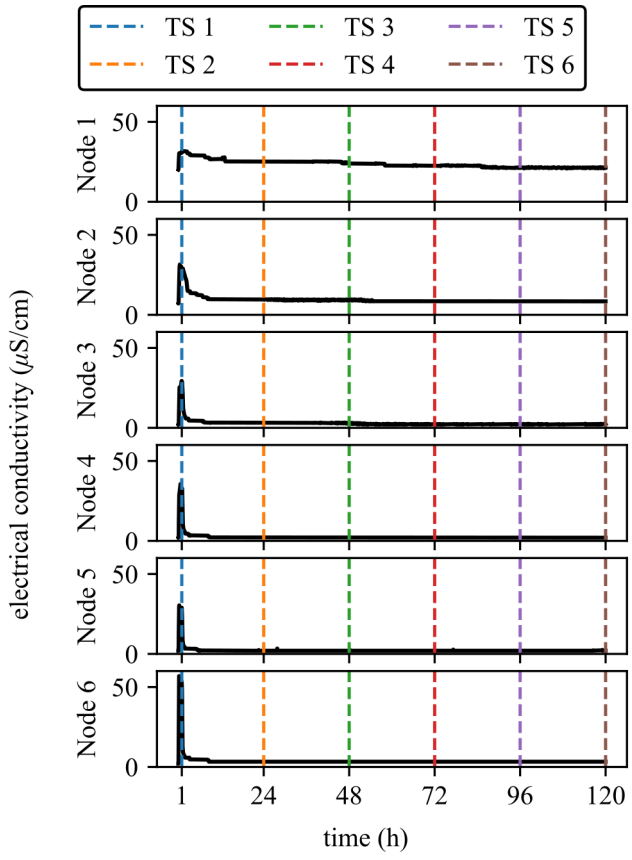

FIGURE 5. The EC of each node over time.

most likely to pool in that area. Due to gravity, the water moves downward as time and water passes. Looking at figure 3, the area underneath is the most dyed by the water, indicating that it is most present at that spot, further supporting why spikes 1 and 2 are recording conductivity for the longest period of time. Note that seepage occurs not far from spike 1 and 2, which must be a result of the high influx of water to the area.

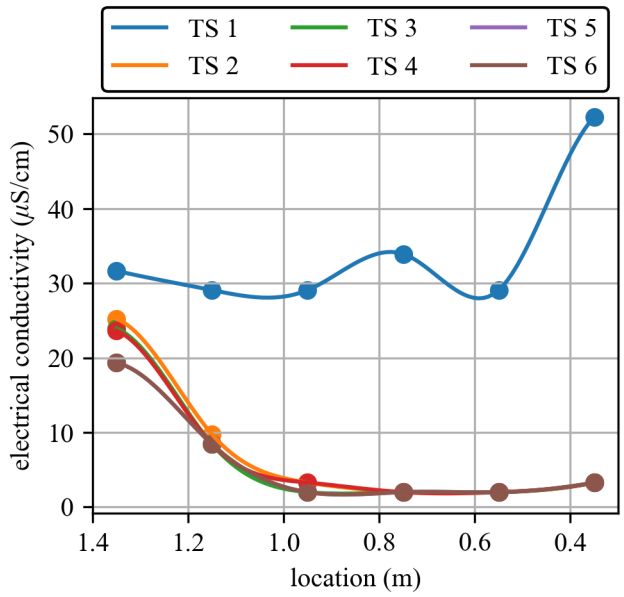

FIGURE 6. The EC at various time intervals with respect to location.

On the other hand, spikes 3, 4, 5, and even 6 dry significantly quicker than spikes 1 and 2. Both of these situations are due to the spikes' respective positions and travel paths of the water. With the rest of the spikes being in more central and higher locations, gravity moves the water downward as it passes through the sand over time.

By displaying the later values, the end of the drying cycle can be better evaluated as well since the spikes have either recorded no conductivity or the battery died by day 6 ($t = 144$). While the test lasted a total of 172 hours, there were no further updates or conductive increases since the previous days, so those values are irrelevant. The batteries in the sensor packages were replaced with fully charged batteries prior to beginning the experiment to effectively test their life.

TABLE 2. Table denoting time stamp values for figures 5 and 6.

Time stamp (TS)	Time (h)
1	1
2	24
3	48
4	72
5	96
6	120

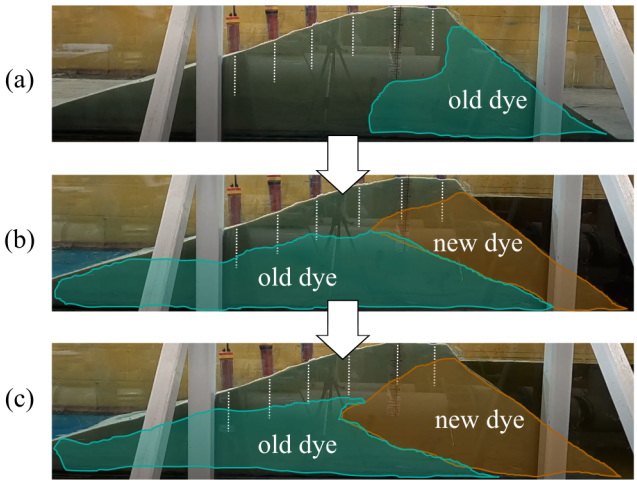

FIGURE 7. Levee saturation tracking using dye deposit movement at times in hours (a) t = 0, (b) t = 0.5, and (c) t = 1 (TS1).

Figure 7 depicts overall water paths throughout the levee. They were interpreted from dye deposits left and carried by the water over time. The prior experiment used blue dye and the discussed experiment uses a reddish-orange dye; therefore, the blue dye gets pushed by the newly incoming orange. White dashed lines represent the length of the sensing spikes from under the package. The tips are the only portion that can detect readings.

The experiment and product have several areas for improvement. The receiver station's design is insecure, relying on a laptop that must remain open and plugged in, risking data loss if power is cut. Additionally, the RF module is connected to the microcontroller with jumper wires, making the system vulnerable to disconnections. A more robust, self-contained setup with sturdier connections, such as solder, screw terminals, or PCB traces, would enhance reliability, along with a backup storage option like SD cards. Future tests will incorporate an upgraded base station. Another limitation is battery life; the spikes lasted only 6–7 days, which is insufficient for continuous outdoor monitoring. Frequent recharging undermines their feasibility as an alternative to levee monitoring networks, necessitating either a more powerful battery or a self-sustaining recharge method like solar cells. Additionally, this experiment did not evaluate the RF module's long-range capabilities beyond 1 meter, though it supports up to 1000 unobstructed meters. In real-world deployments, the receiver may not always be positioned near the embankment. Moreover, the study did not assess sensor package deployment methods or sensor housing durability, which are critical for long-term outdoor applications.

4 CONCLUSION

This experiment demonstrates that the self-contained electrical conductivity sensing spikes can reliably operate for extended periods, accurately measuring and transmitting conductivity data corresponding to realistic levee wetting and drying cycles. The findings confirm that these spikes effectively detect moisture variations, indicating their potential for identifying levee vulnerabilities and structural risks in real time. While certain hardware improvements such as battery capacity and robustness could further enhance their applicability, the presented approach already offers a promising, low-cost alternative to traditional monitoring systems, significantly reducing the need for dense sensor networks without compromising data quality or monitoring reliability.

ACKNOWLEDGMENTS

The authors gratefully acknowledge the financial support of the National Science Foundation through projects CMMI - 2152896, CPS - 2237696, and, ITE - 2344357 The authors' opinions, results, conclusions, and recommendations in this material are their own and do not necessarily reflect the views of the National Science Foundation or the University of South Carolina.

REFERENCES

[1] Tsai, C.-C., Yang, Z.-X., Chung, M.-H., and Hsu, S.-Y., 2022. "Case study of large-scale levee failures induced by cyclic softening of clay during the 2016 meinong earthquake". *Engineering Geology,* ***297***, p. 106518.

[2] Sills, G. L., Vroman, N. D., Wahl, R. E., and Schwanz, N. T., 2008. "Overview of new orleans levee failures: Lessons learned and their impact on national levee design and assessment". *Journal of Geotechnical and Geoenvironmental Engineering,* ***134***(5), pp. 556–565.

[3] Chowdhury, P., Satme, J. N., Flemming, M., Downey, A. R. J., Elkholy, M., Imran, J., and Khan, M. S., 2023. "Stand-alone geophone monitoring system for earthen levees". In Sensors and Smart Structures Technologies for

Civil, Mechanical, and Aerospace Systems 2023, Z. Su, M. P. Limongelli, and B. Glisic, eds., SPIE.

[4] Balistrocchi, M., Moretti, G., Ranzi, R., and Orlandini, S., 2021. "Failure probability analysis of levees affected by mammal bioerosion". *Water Resources Research,* ***57***(12), p. e2021WR030559. e2021WR030559 2021WR030559.

[5] Rebello, L. R. B., Siepman, T., and Drexler, S., 2020. "Correlations between tds and electrical conductivity for high-salinity formation brines characteristic of south atlantic pre-salt basins".

[6] Rusydi, A. F., 2018. "Correlation between conductivity and total dissolved solid in various type of water: A review". *IOP Conference Series: Earth and Environmental Science,* ***118***(1), feb, p. 012019.

[7] Chowdhury, P., Crews, J., Mokhtar, A., Oruganti, S. D. R., Wyk, R. V., Downey, A. R. J., Flemming, M., Bakos, J. D., Imran, J., and Khan, S., 2024. "Distributed real-time soil saturation assessment in levees using a network of wireless sensor packages with conductivity probes". In Volume 11: Safety Engineering, Risk and Reliability Analysis; Research Posters, IMECE2024, American Society of Mechanical Engineers.

[8] Malichi Flemming, Sydney Morris, and Austin R.J. Downey, 2025. Smart penetrometer with edge computing and intelligent embedded systems.

[9] Semiconductor, N., 2007. "nrf24l01 single chip 2.4ghz transceiver product specification".

[10] Hartmut Prautzsch, Wolfgang Boehm, M. P., 2002. "B´ezier-and b-spline techniques".